PHYSICAL REVIEW B VOLUME 39, NUMBER 1 1 JANUARY 1989

Models of flux pinning in the quasistatic limit

A. Brass, H. J. Jensen, and A. J. Berlinsky
Institute for Materials Research, McMaster University, 1280 Main Street West, Hamilton, Ontario, Canada L8S 4M1
(Received 11 July 1988)

The deformations of a two-dimensional vortex lattice pinned by a random pinning potential are studied with use of a molecular-dynamics–annealing method. We find that the response of the lattice varies as a function of the strength of the random potential. For the weakest potentials, the response of the lattice is entirely elastic. For somewhat stronger random potentials, elastic instabilities are induced in the lattice. Further increases in the random potential induce a highly defective lattice, consisting of trapped lattice regions separated by areas in which the lattice flows plastically. By examining the finite-size-scaling behavior of the lattice we conclude that the elastic response is an artifact of the finite size of the simulations and that the strength of the random potential at which the response of the lattice changes from elastic instability to plastic flow goes as $1/\ln(N_v)$, where N_v is the number of vortices in the simulation. Our simulation results are not well described by the theory of Larkin and Ovchinnikov.

I. INTRODUCTION

The problem which we consider is that of a deformable two-dimensional lattice in the presence of a random static potential being acted on by a spatially uniform force which may either be constant in time, or controlled so as to yield a constant center of mass motion of the lattice. The statistical summation of random attractive forces acting on a deformable lattice is a general problem, relevant to flux pinning in type-II superconductors as well as to other phenomena such as the pinning of charge-density waves or Wigner crystals. The nature of the deformations induced by the random potential is of crucial importance to the summation problem. The total force per unit volume from a random potential on a perfectly rigid or only elastically distorted lattice must average out to zero over the shift of the lattice. A finite total pinning force has its origin in the deformations of the lattice as the lattice responds to the random potential.

We have studied the deformations of a simple two-dimensional model by use of computer simulations. A lattice is gradually shifted over a spatially random set of pinning centers. Since our main interest is in the flux-pinning problem, we call the particles in the lattice vortices. As we shift the lattice, we measure the variations in the energy and the pinning force and study the deformations of the lattice. Three different types of response are found as a function of the strength of the random potential.[1]

For very weak pinning, only elastic and reversible deformations of the lattice occur. The total pinning force averaged over shift $\bar{F}$ is zero. However, the size of this weak-pinning region goes to zero as one over the square root of the system size. Hence, this region has no relevance for macroscopic systems.

A narrow intermediate regime exists in which the pinning centers are strong enough to trap a vortex temporarily. Elastic instabilities occur when a pinned vortex suddenly jumps off the pinning center and a new vortex jumps onto the pin. These instabilities produce precipitous drops in the potential energy of the system and $\bar{F}$ becomes finite. This region is elastic, rather than plastic, in the sense that every vortex keeps the same configuration of neighbors during the entire shift.

For somewhat stronger pins, vortices start to become permanently trapped by the pinning centers. Once this occurs plastic flow takes place when the nontrapped vortices flow past the trapped vortices. The motion of the vortices is through a set of channels between the trapped regions. Bottlenecks in the channels cause the flow to pulsate and as a result of these pulsations the potential energy (total force) varies as a periodic, piecewise quadratic (linear) function of the center of the mass. The strength of the random potential at the crossover between the elastic instability and the plastic flow regime is found to decrease only logarithmically as the system increases and so both types of response may be of relevance to finite macroscopic systems.

It is important to note that the values of the pinning potential at which the crossovers from the elastic regime to elastic instability regime and from the elastic instability regime to the plastic flow regimes occur are both functions of the density of the pins. The value of both these crossovers decreases with an increase in the density of the pinning centers. Hence, both the crossovers are collective and not single particle properties of the vortex-pin system.

Our method only allows us to study the static pinning force and the response of the lattice in the limit of a quasistatic drift of the vortex system over the random potential background. In the presence of a driving force above the threshold pinning force, the dynamic pinning force and the detailed response of the lattice might change. However, by performing computer simulations in which we apply a constant pinning force above the threshold pinning force and describe the vortex motion using diffusive dynamics, we find that the classification into the three different types of responses described above still appears to be valid. The comparison of quasistatic to diffusive dynamics is presented at the end of Sec. III D.

The present model has previously been studied numerically by Brandt.[2] Brandt's main concern was to investigate the collective pinning theory of Larkin and Ovchinnikov (LO),[3] which is expected to be applicable to the elastic instability region. Brandt concluded that his simulations did confirm LO's theory, although we believe that Brandt's conclusions may be somewhat optimistic given the results presented in his paper. Although our simulations are much better equilibrated than those of Brandt, we have not been able to find agreement with the predictions of the LO theory.

The paper is organized as follows. In Sec. II we describe the model, our simulation method, and the connection between our method of measuring the pinning force and the model in which the vortices drift with a constant velocity over the pinning centers. In Sec. III we discuss the results obtained from our simulations and attempt to test LO's theory in systems of 1020 vortices. In Sec. IV we discuss the way in which our results scale with the size of the simulation. Finally in Sec. V we discuss the conclusions which can be derived from the computer simulations and their application to flux pinning in real type-II superconductors.

II. MODELS AND METHODS

A. The model

The simulations of the flux-pinning problem are run on a system of N_v vortices with variable positions $\mathbf{r}_i^v$ and N_p fixed attractive pinning centers at random positions $\mathbf{r}_i^p$ in a basic area A with periodic-boundary conditions. We choose a simple Gaussian-like form for the vortex-vortex potential. There are two main reasons for this choice. The first is that it allows us to compare our results with those of Brandt[2] who used this model to test numerically the collective pinning theory of Larkin and Ovchinnikov.[3] The second is that the Gaussian-like potential is short ranged and therefore straightforward to implement in a computer simulation, whereas the true two-dimensional (2D) vortex-vortex interaction is very long ranged, decaying only logarithmically,[4] adding greatly to the complexity of the computer simulations. The intention of this model is not to attempt to simulate a system of vortices in a real type-II superconductor, but rather to provide a simple model system in which to study the interaction of a lattice with a random potential. Following Brandt, the potential energy between two vortices at positions $\mathbf{r}_i^v$ and $\mathbf{r}_j^v$ is written as

$$u_{vv}(r_{ij}) = A_v \left[1 - \frac{r_{ij}^2}{66 R_v^2} \right]^{66} , \tag{1}$$

where

$$r_{ij} = |\mathbf{r}_i^v - \mathbf{r}_j^v|$$

and between a vortex at $\mathbf{r}_i^v$ and a pin at $\mathbf{r}_j^p$ as

$$u_{vp}(r_{ij}) = - A_p \left[1 - \frac{r_{ij}^2}{66 R_p^2} \right]^{66} , \tag{2}$$

where

$$r_{ij} = |\mathbf{r}_i^v - \mathbf{r}_j^p| .$$

The total potential energy of a given configuration of pins and vortices can therefore be written as

$$U = \sum_{\substack{i=1 \\ (i \neq j)}}^{N_v} u_{vv}(r_{ij}) + \sum_{i=1}^{N_v} \sum_{j=1}^{N_p} u_{vp}(r_{ij}) . \tag{3}$$

The length and energy scales for the simulation are set by defining both the ideal vortex lattice constant and the amplitude of the vortex-vortex potential (A_v) to unity. The pinning of the vortex lattice is studied in a similar way to that described by Brandt. The ideal vortex lattice is relaxed in the presence of the pins. This lattice is then shifted over the fixed pins in such a way that it remains properly equilibrated at all times. In this paper we only consider the interaction of the vortex lattice with attractive pins since this is the most physically relevant regime.

B. Relaxation of the vortex lattice

The relaxation of the vortex lattice is achieved using a molecular-dynamics (MD) –annealing method. MD is a widely used algorithm for studying the behavior of dynamical systems of interacting particles.[5] The algorithm makes it possible to follow the path of a system through phase space by integrating the equations of motion numerically for every particle in the system.

In order to use the MD technique we add an auxiliary kinetic term K to the potential and study the behavior of the Hamiltonian

$$H = K + U$$

at very low temperatures. This kinetic term is not supposed to model the true vortex dynamics, but rather to provide a mechanism by which the vortices can explore configuration space and settle into a good local minima on the potential energy surface at low temperatures. The auxiliary kinetic term is defined via

$$K = \tfrac{1}{2} \sum_{i=1}^{N_v} \mathbf{v}_i^2 ,$$

where $\mathbf{v}_i$ is the velocity of the ith vortex, each vortex being assigned a unit mass. The "temperature" of the system is defined to be the average kinetic energy per vortex.

The leapfrog time integration algorithm is used in these simulations, as it is one of the simplest and most accurate of the algorithms available.[6] The algorithm consists of three stages:

(1) Calculate all the forces on the particles at time t.

(2) Calculate the particle velocities at time $t + \frac{1}{2}\delta t$ using

$$v(t + \tfrac{1}{2}\delta t) = v(t - \tfrac{1}{2}\delta t) + \frac{F(t)}{m} \delta t . \tag{4}$$

(3) Calculate the positions at time $t + \delta t$ using

$$x(t + \delta t) = x(t) + v(t + \tfrac{1}{2}\delta t)\delta t . \tag{5}$$

At the start of the relaxation run the vortices are placed at their ideal lattice site positions and given a ran-

dom velocity chosen from a Gaussian distribution. The simulation is then run at a temperature of $0.1A_p$. The temperature during this run is kept constant by rescaling the vortex velocities at the end of each timestep so that the total kinetic energy remains constant. For the first few hundred timesteps the potential energy of the system decreases as the vortices relax about the pins. Eventually, however, the total potential energy tends towards a constant value. Once this point has been reached, the temperature of the vortices is decreased, and the system is reequilibrated. This whole process is repeated several times until the simulation is at a temperature of typically $10^{-4}A_p$. Once the potential energy has stabilized at this temperature the temperature rescaling is switched off and the system is allowed to reach equilibrium in the microcanonical ensemble. The major difference between this relaxation method and the one used by Brandt is that while Brandt attempts to minimize the potential energy directly, the MD annealing method subtracts energy from the system in the form of kinetic energy, the system then repartitioning the energy between kinetic and potential energy by following the equation of motion.

During the relaxation procedure the vortex-pin system shows some behavior not normally seen in an MD simulation. In a typical MD simulation the center of mass of the interacting particles remains constant (as there is no external force on the system). However, the center of mass of the vortices is seen to oscillate slowly about a fixed value. This oscillation is due to the fact that the whole system consists of the vortices and the pins, not just the vortices. Any change of the center of mass of the vortices changes the total vortex-pin potential energy. At any finite temperature T the center of mass of the vortices will oscillate about the minimum of this potential such that the energy stored in the oscillation is kT. Typically the amplitude of this mode is very small. However, for the weakest pins, the elastic constant for this mode is small, as the pins can only exert a weak restoring force. In this case the amplitude of the vibration can be a significant proportion of the vortex-vortex spacing.

C. Measurement of the pinning force

After the vortex lattice has been relaxed, its center of mass is shifted over the pins in the $\langle 1,0\rangle$ direction by successively adding a small displacement δx to each of the vortices. After each shift by δx the lattice is relaxed using the MD algorithm. During this relaxation the temperature of the vortices is kept constant by rescaling the vortex velocities, and any net linear momentum of the vortex lattice is removed by adding an equal and opposite velocity to each of the vortices. From Eq. (4) it can be seen that keeping the net linear momentum zero is equivalent to always applying an external homogeneous driving force so as to exactly balance the force that the pins exert on the vortices. In order that the vortex lattice remains properly relaxed after each shift it is important that, firstly, sufficient MD steps are run between the shifts so that the vortex potential is properly minimized and, secondly, that δx is not so large that the vortex configuration is shifted too far from the local minima of the potential-energy surface. The total cumulative shift of the vortex lattice center of mass is typically one lattice spacing.

The number of MD steps needed to equilibrate the lattice after each shift can be determined in a straightforward manner. Several jobs are run from the same starting configuration, each run having a different number of MD relaxations between shifts. The number of relaxations needed is simply given by the minimum number of MD steps between shifts such that increasing the number of relaxations does not significantly alter the path that the configurations take through phase space. The number of MD relaxations between each shift typically varies between four per shift for the weak pins to 10 per shift

In the absence of an external force, and when the kinetic energy is negligible, equilibrium configurations satisfy

$$\frac{\delta U}{\delta \mathbf{r}_i}=0 \text{ for all } i \ ,$$

where U is given by Eq. (3). If the center of mass is shifted by

$$\delta \mathbf{X}=\frac{1}{N_v}\sum_{i=1}^{N_v}\delta \mathbf{r}_i$$

and held fixed, then equilibrium is determined by minimizing

$$\bar{U}=U+\mathbf{f}\cdot\sum_{i=1}^{N_v}\mathbf{r}_i \ ,$$

where $\mathbf{f}$ is adjusted to yield the correct value of $\delta\mathbf{X}$. Then

$$\delta\bar{U}=0 \Longrightarrow \mathbf{f}=-\frac{\delta U}{\delta \mathbf{r}_i} \text{ for all } i \ .$$

The change in the total potential energy is

$$\delta U=\sum_{i=1}^{N_v}\frac{\delta U}{\delta \mathbf{r}_i}\cdot\delta\mathbf{r}_i=-\mathbf{f}\cdot\sum_{i=1}^{N_v}\delta\mathbf{r}_i=-N_v\mathbf{f}\cdot\delta\mathbf{X}=-\mathbf{F}\cdot\delta\mathbf{X} \ , \tag{6a}$$

where $\mathbf{f}$ is the total external force on the vortex lattice. In equilibrium, the force $\mathbf{F}$ exactly balances the total pinning force

$$\mathbf{F}=-\sum_{i,k}\frac{\delta U_{vp}(r_{ik})}{\delta \mathbf{r}_i} \ . \tag{6b}$$

The result that $-\mathbf{F}\cdot\delta\mathbf{X}=\delta U$ is the change in potential energy of the lattice holds if the system has equilibrated, provided that it did not jump from one metastable minimum of $\bar{U}$ to another while its center of mass moved by $\delta\mathbf{X}$. The fact that the force $\mathbf{F}$ and the change in the potential δU are measured separately provides a check that the system is well equilibrated. In the case of elastic instabilities, where the system *does* jump between metastable minima of $\bar{U}$, Eq. (6a) does not apply. The above results can be used to determine the size of the incremental shift we apply to each vortex. The value of δx used in

the simulations is the largest one such that Eq. (6a) is satisfied. For weak pins we find that δx should be about 10^{-3} (in units of the lattice spacing), whereas for strong pins it should be reduced to 10^{-4}.

Four quantities are measured and recorded after each incremental shift of the vortex lattice: the average vortex-vortex potential energy U_{vv}, the average vortex-pin potential energy U_{vp}, the total pinning force F, and the spatial fluctuations in the total force on each pin W:

$$U_{vv}=\frac{1}{N_v}\sum_{\substack{i,j=1\\(i\neq j)}}^{N_v} u_{vv}(r_{ij}) , \tag{7a}$$

$$U_{vp}=\frac{1}{N_v}\sum_{i=1}^{N_v}\sum_{j=1}^{N_p} u_{vp}(r_{ij}) , \tag{7b}$$

$$F=\frac{1}{N_v}\sum_{i=1}^{N_v}\sum_{j=1}^{N_p} F_{vp}(r_{ij}) , \tag{7c}$$

where $F_{vp}(r_{ij})$ is the force between a vortex at $\mathbf{r}_i^v$ and a pin at $\mathbf{r}_j^p$, and

$$W=\frac{1}{N_v}\sum_{i=1}^{N_p} F_p^2(r_i^p) , \tag{7d}$$

where $F_p(r_i^p)$ is the total force on pin i. The vortex configurations are periodically written onto disc during the shifting procedure.

The method of successively shifting and relaxing the lattice can be related to the process in which the lattice moves with a small constant center-of-mass velocity over the pinning centers. The two processes are equivalent in the case where the particles in the lattice follow a diffusive equation of motion. This procedure should thus be relevant to type-II superconductors where the vortex motion is believed to follow diffusive dynamics.[7]

To make the connection between the two methods, we consider the equation of motion

$$\eta\frac{d\mathbf{r}_i}{dt}=\mathbf{f}_{Dr}+\mathbf{f}_{vv}^i+\mathbf{f}_{vp}^i . \tag{8}$$

Here $\mathbf{f}_{vv}^i$ is the total force exerted on vortex i from all the surrounding vortices, $\mathbf{f}_{vp}^i$ is the total pinning force felt by this vortex, and η is the friction coefficient. By choosing the driving force $\mathbf{f}_{Dr}$, to be given by

$$\mathbf{f}_{Dr}=\mathbf{f}_0-\frac{1}{N_v}\sum_{i=1}^{N_v}\mathbf{f}_{vp}^i ,$$

where $\mathbf{f}_0$ is a constant, the vortex system will drift slowly over the pins with a constant center-of-mass velocity equal to $\mathbf{f}_0/\eta$. If $\mathbf{f}_0$ is chosen small enough, the vortex configuration will always be kept close to the minimum configuration (of $U_{vv}+U_{vp}$) due to the term $\mathbf{f}_{vv}^i+\mathbf{f}_{vp}^i$ in Eq. (8). It is, however, difficult numerically to relax the potential by the discrete version of Eq. (8) since this equation corresponds to a relaxation along the gradients. In this respect molecular dynamics annealing is much more efficient. The equivalence between the two techniques is demonstrated in Sec. III D.

It seems natural, as suggested by Brandt,[2] to identify the maximum static pinning force with the pinning force averaged over the position of the center of mass

$$\bar{F}=\lim_{L\to\infty}\left[\frac{1}{L}\int_0^L F(X)dX\right] . \tag{9}$$

By this definition of $\bar{F}$ it follows that $\bar{F}$ times a displacement $\Delta X_{\text{c.m.}}$ will, on average, be equal to the work needed to translate the vortex system, when the translation is done by a force that at any instant is exactly able to overcome the restoring pinning force. This feature makes it plausible to assume that $\bar{F}$ will be approximately equal to the threshold pinning force measured for a macroscopic system. Furthermore, the pinning force defined by Eq. (9) will be given by the instabilities induced by the random-pin potential. These elastic or plastic instabilities produce discontinuities in the potential energy as function of the center-of-mass (c.m.) position $U(X)=U_{vv}(X)+U_{vp}(X)$. By using $F(X)=dU/dX$ (this equation holds also in the case of diffusive dynamics) we obtain

$$\bar{F}=\lim_{L\to\infty}\left[\frac{1}{L}\left[U(L)-U(0)+\sum_{x_i\in[0,L]}\text{disc}U(x_i)\right]\right]$$
$$=\lim_{L\to\infty}\left[\frac{1}{L}\sum_{x_i\in[0,L]}\text{disc}U(x_i)\right]$$

where the sum is over the discontinuities

$$\text{disc}U(x)=\lim_{\epsilon\to 0^+}[U(x+\epsilon)-U(x-\epsilon)]$$

within the interval $[0,L]$. Hence, the force defined in Eq. (9) will, when calculated in the limit of a quasistatic shift, only depend on inherent elastic and plastic properties of the vortex-pin system.

D. Computational details

The lists giving all the vortex-vortex and vortex-pin interactions are calculated using the linked-list algorithm described by Hockney and Eastwood.[6] All the simulations are run on a Floating Point System FPS-264 processor and a Cray Research, Inc. X-MP/24 supercomputer.

III. RESULTS

A. Introduction

The flux line lattice is found to exhibit three qualitatively different types of behavior as the center of mass of the vortices is shifted over the pins. For weak pins the response of the vortex lattice (VL) is entirely elastic, the average pinning force over a shift of one lattice spacing being several orders of magnitude smaller than the maximum pinning force measured over the shift. For stronger pins (or a higher pinning density, or a higher value of R_v, or a larger system) the average pinning force becomes comparable with the maximum pinning force. Although none of the vortices become trapped on the pins for an entire shift of the center of mass by a lattice

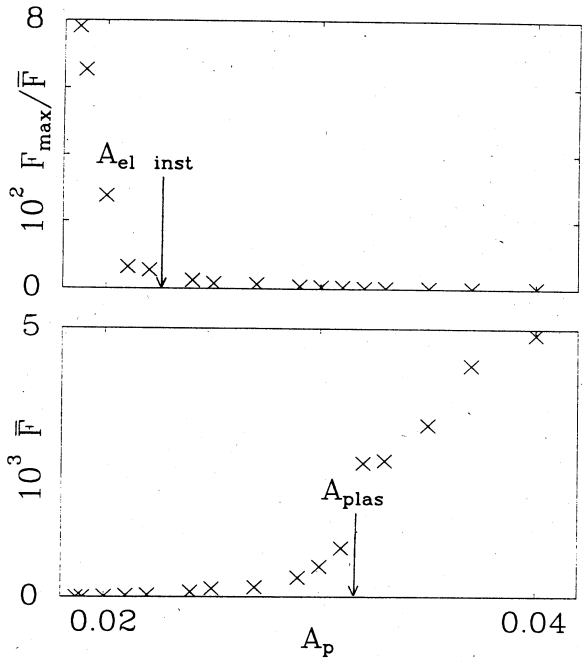

FIG. 1. $\bar{F}$ and $F_{max}/\bar{F}$ as a function of A_p for a system of 340 vortices with $R_v=0.6$, $R_p=0.25$ and $N_p=146$.

spacing, some vortices are briefly trapped causing elastic instabilities. Finally, for even stronger pins, some vortices are permanently trapped on the pinning centers. With some of the vortices fixed, the remaining vortices must flow plastically around them as the center of the mass of the VL is shifted.

Figure 1 shows graphs of $\bar{F}$ and $F_{max}/\bar{F}$ as a function of A_p for a system of 340 vortices with $R_v=0.6$ and 146 pins with $R_p=0.25$, where $\bar{F}$ and F_{max} are the average and maximum pinning forces measured over a shift of the center of mass of the vortices by one lattice spacing. From these graphs it can be seen that the value of A_p at which $F_{max}/\bar{F}$ falls to a constant is lower than the value of A_p at which the value of $\bar{F}$ begins to rise rapidly. By examining the vortex configurations it is clear that the rapid rise in $\bar{F}$ is associated with the onset of plastic flow and the trapping of vortices (for values of $A_p>0.032$ at least one vortex was trapped for the entire shift of the lattice). Similarly the rapid fall in the value of $F_{max}/\bar{F}$ can be associated with the crossover from the elastic regime into the elastic instability regime. For a given set of values of R_p, R_v, the pinning density and the system size,

TABLE I. The values of $A_{el\ inst}$ and A_{plas} measured on a system of 340 vortices for a range of model parameters.

R_v	R_p	N_p	$A_{el\ inst}$	A_{plas}
0.6	0.25	340	0.016	0.021
0.6	0.25	146	0.024	0.032
0.6	0.25	73	0.03	0.05
0.6	0.25	1	0.08	0.15
0.75	0.25	146	0.007	0.013
0.75	0.25	73	0.013	0.021
0.6	0.50	146	0.08	0.138
0.75	0.50	146	0.018	0.052

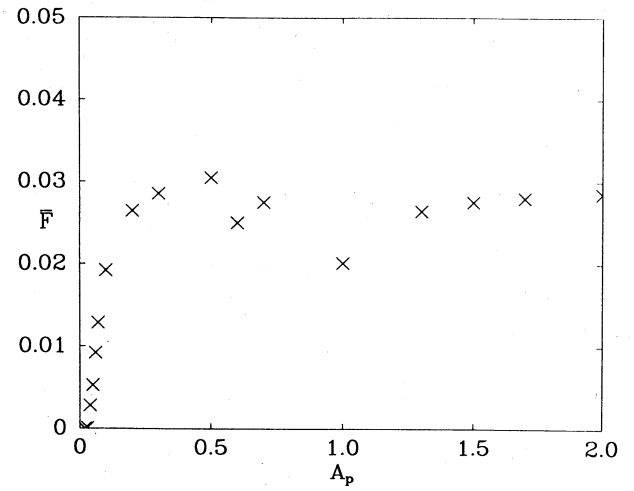

FIG. 2. $\bar{F}$ as a function of A_p for a larger range of A_p than Fig. 1.

we can therefore define two quantities: $A_{el\,inst}$, which labels the value of A_p at which the lattice crosses over from the elastic to the elastic instability regime, and A_{plas}, which labels the value of A_p at which the lattice crosses over from the elastic instability to the plastic regime. Table I shows the various values of $A_{el\,inst}$ and A_{plas} obtained for a range of model parameters for a system consisting of 340 vortices.

The values for $A_{el\ inst}$ and A_{plas} given in this table are not exact as each value quoted refers to a particular pin configuration, not an average over pin configurations. However there are certain trends in the behavior of the VL that can be determined from this data. First we can see that values of $A_{el\ inst}$ and A_{plas} depend on the density of the pinning centers, decreasing the pin density increases the values of A_p at which the crossovers occur, the value of $A_{el\ inst}$ scaling as $\sqrt{1/N_p}$. This suggests that elastic instabilities and vortex trapping are not caused by individual pinning centers but involve the cooperative action of several pinning centers coupled through the VL. Secondly we can see that, as we would expect, reducing c_{66}—the shear modulus—by increasing R_v reduces the values of A_p at which the crossovers occur.

Figure 2 shows how the pinning force varies with A_p for a larger range of values A_p than those given in Fig. 1. Figure 3 shows the same data plotted on log scales. From these graphs we can see that for values of A_p larger than A_{plas} the pinning force rises rapidly before reaching a maximum and settling down to a constant value. It should be noted that the dependency of $\bar{F}$ on A_p is different from the one found by Brandt.[2] Brandt typically found that $\bar{F}$ scaled as A_p^2 for $0.01<A_p<0.1$. We see no clear sign of such a region in our simulations.

As the value of A_p is increased (with the other model parameters held constant) the VL becomes increasing disordered. This increasing disorder can be seen in the initial relaxed VL's (the VL's we obtain from our initial MD anneal in the presence of the pinning centers). Figure 4 shows how the number of miscoordinated vortices

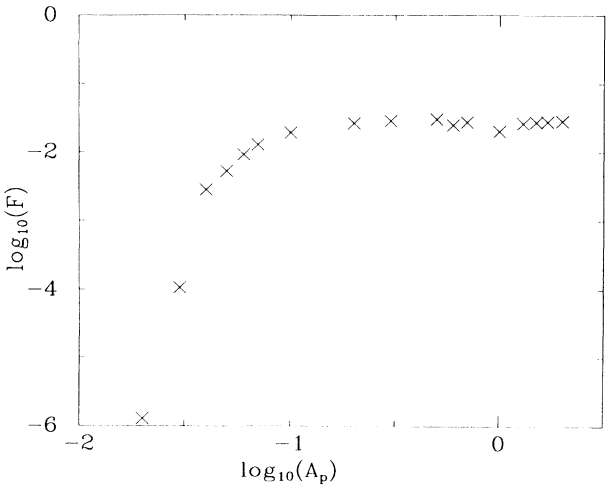

FIG. 3. $\log_{10}(\bar{F})$ vs $\log_{10}(A_p)$. Note that this graph does not have an initial slope of 2.

varies with A_p. It can be seen from this graph that the number of induced defects rises rapidly at some critical value of A_p and then levels off when the fraction of defective vortices in the lattice reaches about 30%. The value of A_p at which defects start to be created is very close to A_{plas}. Every relaxed configuration that contains defects will flow plastically when shifted over the pinning centers.

This increasing disorder can also be seen in the vortex-vortex radial distribution functions. Figure 5 shows the radial distribution functions for various values of A_p for a system with $A_{\text{plas}}=0.032$. It can be seen from these functions that increasing the value of A_p decreases the degree of positional correlation. For values of A_p larger than A_{plas} the radial correlation functions resemble those obtained from a liquid, the correlation decaying to 1 after only 4 lattice spacings.

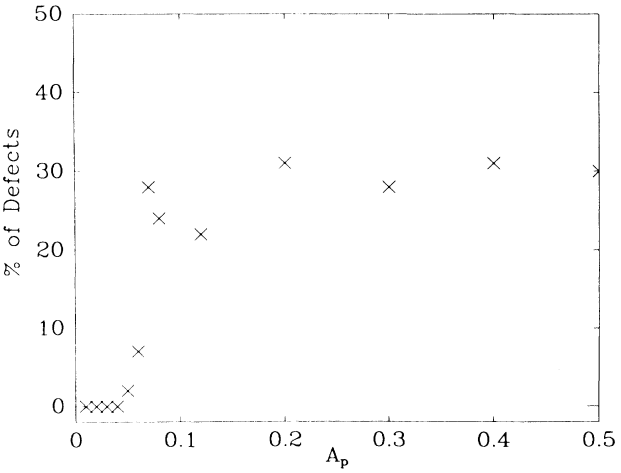

FIG. 4. Percent of defective vortices as a function of A_p for a system of 108 vortices with $R_v=0.6$, $R_p=0.25$, and $N_p=46$.

B. Elastic regime

Figure 6 shows the various potentials and forces as a function of center-of-mass displacement for a lattice in the elastic regime. In this regime all the properties vary smoothly and periodically as a function of the center-of-mass position with a period equal to the lattice spacing. The pinning force averaged over a shift of one lattice spacing $\bar{F}$ is much less than the maximum pinning force over the shift $F_{\max}$. The distortion of the lattice is reversible, and all the vortices are coordinated by the same six neighbors for all values of the center-of-mass displacement. Table II lists the results obtained from the elastic lattices. It is interesting to note that the maximum pinning force obtained increases with increasing N_p until it reaches some maximum value and then starts to decrease with further increases in N_p. The decrease in $F_{\max}$ as a function of N_p results from the fact that, as the number of pinning centers increases, the random potential produced by these centers becomes more homogeneous thereby reducing the net pinning force on the VL.

C. Elastic instability regime

Figure 7 shows the various potentials and forces as a function of center-of-mass displacement for a lattice in the elastic instability regime. The characteristic feature of the runs in this regime is that, while the potential, etc., are still periodic with periodicity equal to the lattice spacing, they are no longer smooth, but contain discontinuities. These discontinuities were not observed by Brandt, presumably because his relaxation algorithm was not sufficiently accurate (see Sec. III D). The discontinuities in these curves can be associated with vortices being temporarily trapped by pinning centers. As the shift of the lattice continues, the elastic distortion in the lattice caused by the pinned vortex increases until the trapped vortex suddenly escapes from the pin, typically to be replaced by another vortex. This process can most easily be seen in the case of a VL with a single pinning center.

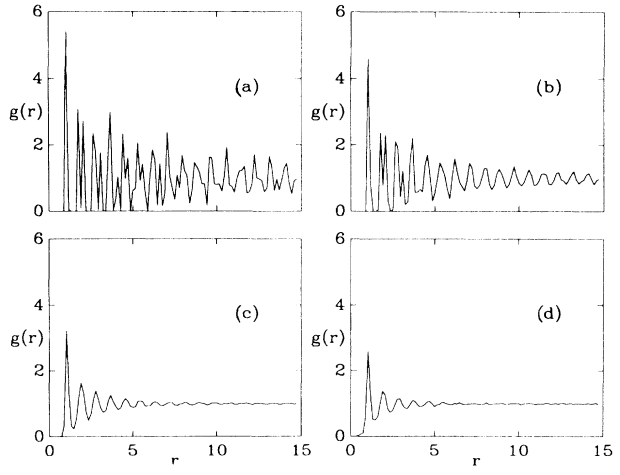

FIG. 5. Vortex-vortex radial distribution functions for a system of 340 vortices with $R_v=0.6$, $R_p=0.25$, and $N_p=146$. (a) $A_p=0.01$, (b) $A_p=0.03$, (c) $A_p=0.1$, (d) $A_p=0.5$.

TABLE II. Numerical results for a system of 340 vortices in the elastic regime for a range of model parameters. $U_{\min}$ is the lowest value of the total vortex potential observed over the shift. U_{ht} measures the difference between the minimum and maximum values of the total vortex potential. $F_{\max}$ is the maximum value of the pinning force observed over the shift.

R_v	R_p	A_p	N_p	$U_{\min}$	U_{ht}	$F_{\max}$
0.6	0.25	0.01	1	0.17604	3×10^{-5}	9×10^{-5}
0.6	0.25	0.01	73	0.17543	18×10^{-5}	50×10^{-5}
0.6	0.25	0.01	146	0.17480	20×10^{-5}	70×10^{-5}
0.6	0.25	0.01	340	0.17345	12×10^{-5}	40×10^{-5}
0.6	0.125	0.005	146	0.17590	8×10^{-5}	30×10^{-5}
0.6	0.25	0.005	146	0.17544	11×10^{-5}	40×10^{-5}
0.6	0.50	0.01	146	0.17213	6×10^{-5}	20×10^{-5}
0.75	0.25	0.005	146	0.50736	10×10^{-5}	40×10^{-5}
0.75	0.25	0.01	73	0.50728	20×10^{-5}	80×10^{-5}

Figure 8(a) shows the initial configuration with a vortex directly on top of the pinning center. As the shift continues the strain field about the pinned vortex increases rapidly, extending across the full width of the sample [Fig. 8(b)]. Once the energy stored in the strain field reaches a critical value the trapped vortex suddenly hops off the pinning center to be replaced by another vortex [Fig. 8(c)]. The fact that this depinning-pinning phenomena can be described as a hop can be seen by examining the trajectories of the two vortices which hop and onto the pin during the shift (Fig. 9). These vortices are denoted by the bold circles in Fig. 8. By examining Figs. 8(b) and 8(c), it can be seen that the pinning force changes sign directly after the hop. By further shifting the lattice we finally reach a configuration in which every vortex has been displaced by one lattice spacing from its start position. Figure 10 shows the various potentials and forces as a function of center of mass for this process. At no point in this process are defects created in the lattice (defects being defined as vortices with a coordination number different from 6).

It should be noted that although the pinning-depinning events occur on single pinning sites, they arise as a collective effect of the pins. The onset of the elastic instability region is strongly dependent on the pinning density. For example, in a system of 340 vortices with $R_v=0.6$ and $R_p=0.25$ and $N_p=1$, elastic instabilities will be induced if $A_p \geq 0.08$. Whereas, with 146 pinning centers pinning-depinning events can be induced with A_p as small as 0.024. In Sec. IV we also show that, for a fixed density of pins, the value of $A_{\text{el inst}}$ scales as $1/\sqrt{N_v}$. Therefore for a macroscopic sample, any pins, however weak, will induce elastic instabilities.

D. Plastic flow regime

Figure 11 shows some typical force and potential curves for a system in the plastic regime. It is clear that these curves are no longer periodic with periodicity of the lattice spacing. All the curves show a characteristic sharp saw-toothed form with many discontinuities. In this regime some of the vortices remain trapped on the pinning centers for the entire shift, the abrupt drops in the potential energy being associated with the plastic flow about these trapped vortices. Figure 12 shows the flow of the vortices for the same run as in Fig. 11. This figure shows that, for these particular model parameters, the majority of the lattice is trapped, the moving vortices flowing in well-defined channels with a width of one lattice spacing. For other values of the model parameters these channels can be much wider (Fig. 13). The VL can now be highly defective. Figure 14 shows the initial relaxed lattice used in the run described by Fig. 11, the coordination number of the vortices being calculated using the Voronoi polygon construction.[8] For some runs as many as half the vortices can have coordination numbers different from six. However, there is no clear connection between the channels and the position of the miscoordinated vortices. Similarly by examining the configurations as the VL is shifted, we see no sign of any clear connection between the total potential energy and the number of defective vortices in the VL.

The sharp saw-toothed shape of the force curve can only be obtained if the lattice is sufficiently well relaxed during the shift over the pins. Less complete relaxation gives the same type of force curves as those obtained by Brandt. This is illustrated in Fig. 15 where the force curves for completely relaxed (curve B) and incompletely relaxed (curve A) simulations are shown. Curve A is very similar to the results presented by Brandt for the same parameters (but presumably for a different set of random pin positions). The criterion for complete relaxation defined by Eq. (6), i.e., that dU/dX should equal $F(X)$ (where X is the center-of-mass coordinate), is satisfied by curve B but not by curve A.

As the center of mass of the vortices is shifted, the total potential energy increases quadratically with a corresponding linear increase in the pinning force. The pinning force increases until it reaches a critical value at which point the lattice undergoes a sudden reorganization which releases some of the accumulated potential energy in the VL. The quadratic increase in the VL potential energy then resumes. Each linear section of the $F(X)$ curve has approximately the same slope and reaches the same maximum value for a given set of model parameters. The release of potential energy in the VL is linked to the flow of the vortices in channel-like paths between the trapped vortices, the drop coinciding with a sudden increase in the flow. The successive smooth increases and sudden drops in the pinning force can be associated with

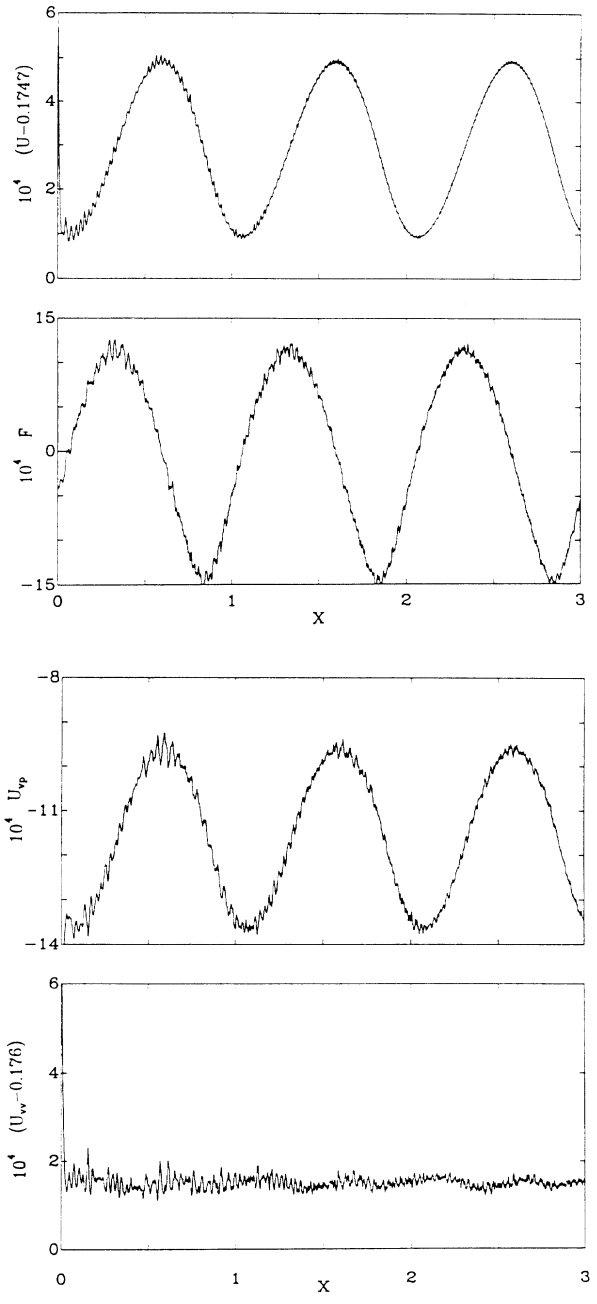

FIG. 6. $U(X)$, $F(X)$, $U_{vv}(X)$, and $U_{vp}(X)$ [where $U(X)=U_{vv}(X)+U_{U_{vp}}(X)$] for a system of 340 vortices with $A_p=0.01$, $R_v=0.6$, $R_p=0.25$, and $N_p=146$. The high-frequency noise is caused by thermal fluctuations.

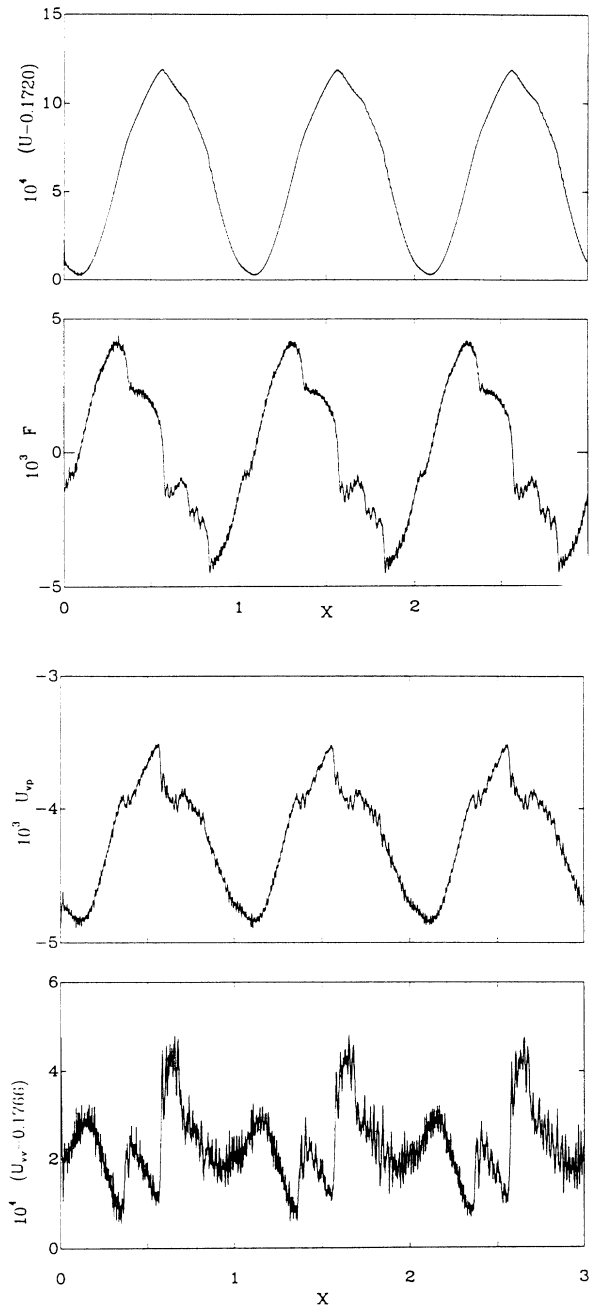

FIG. 7. $U(X)$, $F(X)$, $U_{vv}(X)$, and $U_{vp}(X)$ for a system of 340 vortices with $A_p=0.028$, $R_v=0.6$, $R_p=0.25$, and $N_p=146$.

a pulsating flow through the channels. The variations in $U(X)$ and $F(X)$ can be remarkably periodic (see Fig. 11) with a periodicity specific to the channel in operation, the periodicity can change when one channel closes and a new one opens. The width of the flowing channels depends on the strength of A_p. If A_p is only slightly larger than A_{plas} then the width of the flowing regions is large. As A_p is increased, the width of the channels decreases, until for values of A_p corresponding to the plateaux in $\bar{F}$ (see Fig. 2) the width of the channel is only a single lattice spacing. For this case the periodicity in $F(X)$ and $U(X)$ corresponds to vortices in the channel moving a lattice spacing. Examining the configurations it can be seen that there are bottlenecks in the channel and that the drops in $U(X)$ occur when a single vortex is pushed through one of these bottlnecks. Table III shows some of the numerical results obtained from simulation runs in the plastic regime for a range of model parameters. Several qualitative features of the pinning region can be deduced from this table. First, as demonstrated in Fig. 2, the maximum value of the pinning force is independent of the value of A_p. However, the derivative of the linear parts of the

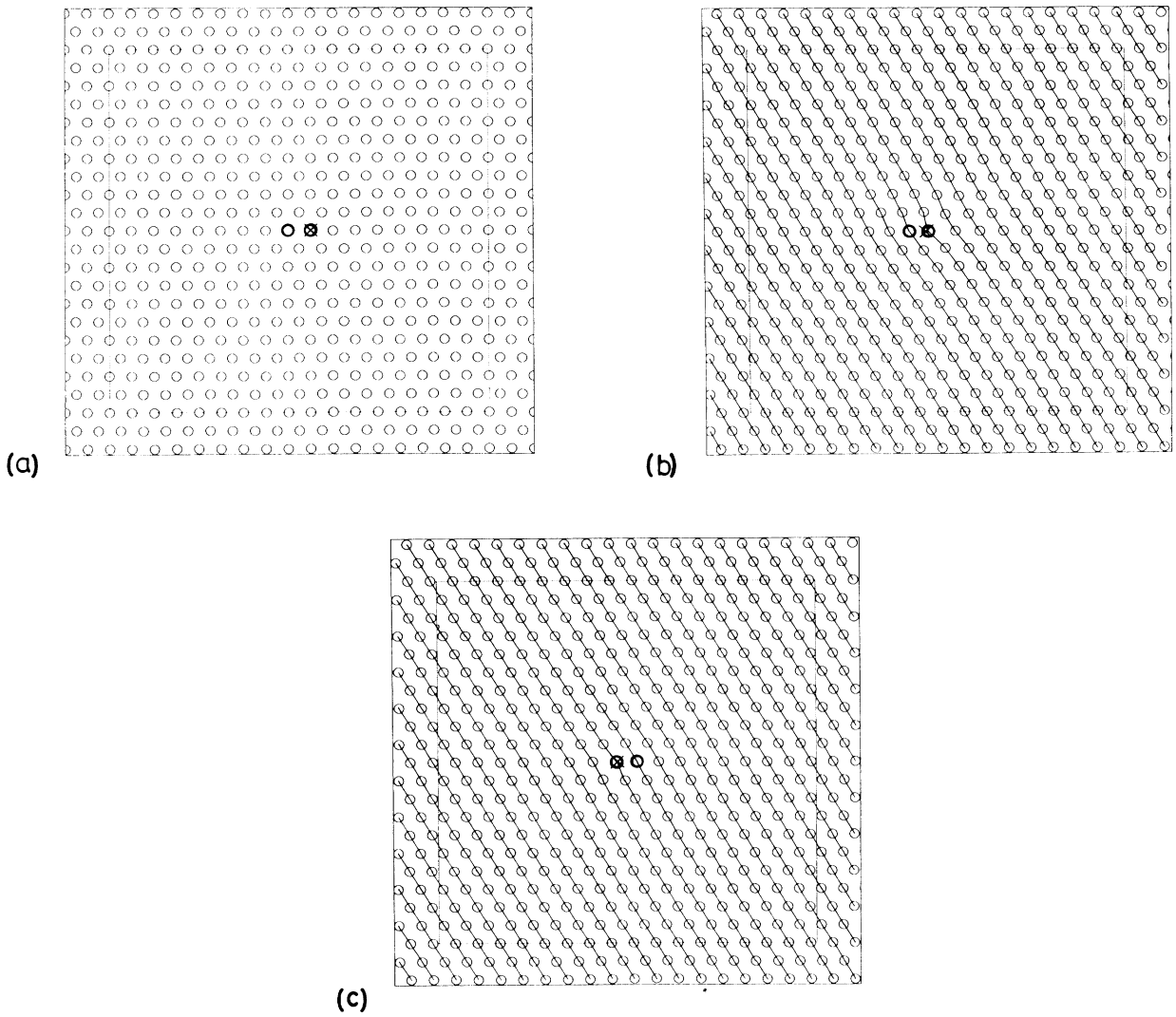

FIG. 8. A series of configurations showing the development of an elastic instability for a system of 340 vortices with $N_p=1$, $R_v=0.6$, $R_p=0.25$. The dashed lines show the extent of the computational box. The vortices are shifted from left to right. Two of the vortices are shown in heavier type; the vortex located on the pinning center in the relaxed configuration, and the vortex that eventually hops onto the pinning center. The cross shows the position of the pinning center. (a) The relaxed vortex configuration. (b) The configuration just before the vortex on the pin hops off. The lines are drawn on the figure as a guide to the eye to show the extent of the strain field produced by the pinned vortex. (c) The configuration just after the vortex hop. Note that most of the strain energy stored in the system has now been released.

pinning force versus center of mass k is weakly dependent on A_p. Increasing A_p from 0.1 to 1.0 typically raises k by a factor of approximately 2. As would be expected there seems to be a similar dependence of the difference between the maximum and minimum values of the potential U_{ht} with A_p. The values of U_{ht}, $F_{\max}$, and k depend also on the pinning density and the value of R_v. Increasing the pinning density increases the values of all these quantities, as does reducing R_v. Similarly, by increasing R_p we can also increase U_{ht}, k, and $F_{\max}$.

It is possible to compare the results obtained using the shift and relax algorithm with those obtained using a constant excess driving force and diffusive dynamics. The comparison between the two methods is shown in Fig 16. In this figure we compare the pinning force and potential obtained as a function of the center-of-mass coordinate for two different simulations: the first for a run in which we use the successive shift and relax algorithm, and the second in which we use diffusive dynamics and an excess driving force of 10^{-4}. The two runs show qualitatively the same features. Both contain piecewise linear pinning forces as a function of center of mass, both contain precipitous drops in the potential and force curves, both give similar values of $\bar{F}$, and in both runs the moving vortices flow through well-defined channels separating regions of trapped vortices. The two sets of curves are not identical, but we would not expect them to be. First, the two different runs are made with different dynamics and the shift and relax method contains a noise term (temperature) which is not included in the diffusive dynamics. Be-

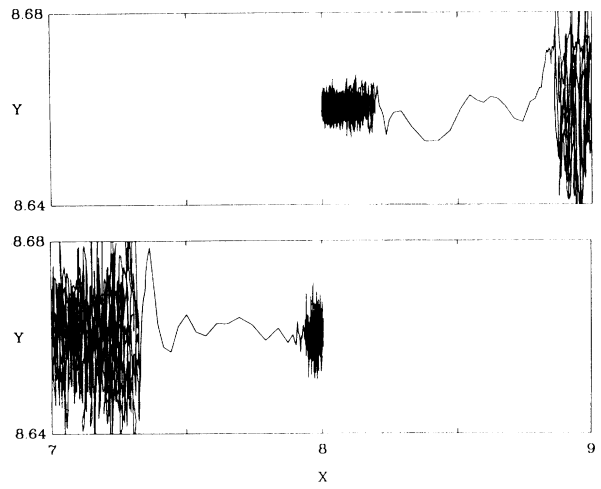

FIG. 9. The top curve shows the trajectory of the vortex that is initially localized by the pinning center as the shift of the center of mass procedes. The bottom curve shows the trajectory of the vortex that hops onto the pinning center.

cause of these differences we would not expect the vortices in the two different simulations to follow the same trajectories. Second, we are not yet in the limit of the excess driving force being zero. This can be seen in the fact that precipitous drops in the potential and pinning force are smaller in the run made using diffusive dynamics than in the run made by successively shifting and relaxing the lattice. Nevertheless the two runs are qualitatively very similar.

E. Connection to Larkin-Ovchinnikov theory

Random-pinning centers destroy the long-range oder of the VL.[9] In the LO summation theory it is assumed that there remains short-range order of the VL inside a "coherence area," an area within which the VL is assumed to be only elastically distorted. The total pinning force is assumed to be due to the statistical fluctuations of the pinning force inside these areas. As LO summation theory assume that the lattice is only distorted elastically inside finite areas, we might expect the theory to hold within the elastic instability regime of our model. We would not expect the LO summation theory to hold for the elastic flow regime as the pinning force in this case is solely due to finite-size effects within our model, equivalent to the correlated areas being much larger than the system size. The elastic regime is expected to vanish for any macroscopic sample. Similarly we would not expect LO to hold in the plastic flow regime as in this case the VL is highly defective and plastically deformed. One of the major predictions of the LO summation theory is that the pinning force, $\bar{F}$ should be proportional to the fluctuations in the pinning force $\overline{W}$

$$\bar{F}=\frac{c\overline{W}}{c_{66}R_p}\ , \tag{10}$$

where c is some constant. In the LO theory it is possible to estimate A_c, the strength of the pinning potential at which the size of the correlated area becomes smaller than the simulation size[2]

$$A_c=\frac{2.026R_p}{\sqrt{N_p}}\ , \tag{11}$$

where we have assumed that $R_p \leq 0.25$ and taken $R_v=0.6$. In order to test the LO theory in our simulation we need to find a parameter set such that $A_c < A_{\text{plas}}$. For example, consider a system of 1020 vortices with $R_v=0.6$ (for which $c_{66}=0.2695$), and 438 pins with $R_p=0.25$. For this system $A_{\text{el inst}}\approx 0.015$, $A_c\approx 0.024$, and $A_{\text{plas}}\approx 0.031$. Therefore for values $0.024 \leq A_p \leq 0.031$ we might expect the LO theory to be applicable. Figure 17 shows the values of $\bar{F}/\overline{W}$ obtained for various values of A_p with a different pin configuration being used for each run. The values of $\bar{F}$ and $\overline{W}$ are obtained by averaging F and W, respectively [cf. Eqs. (7)] over a shift of the center of mass of the VL by one lattice spacing. Although there is a good degree of scattering in our data, it does not seem consistent with Eq. (10), we do not find that $\bar{F}/\overline{W}$ is constant. This could be due to finite-size effects, perhaps the size of the correlated areas is larger than is given by Eq. (11), perhaps we need to be able to fit several correlated volumes into the simulation area before the averages work properly. Our data appears to be consistent with $\bar{F}/\overline{W}\rightarrow 0$ as $A_p \rightarrow A_{\text{el inst}}$ suggestion that $\bar{F}/\overline{W}$ cannot be a constant and that the transition of the lattice from the elastic to the elastic instability regimes is

TABLE III. Numerical results for a system of 340 vortices in the plastic regime. k is the derivative of the linear parts of the pinning force vs center-of-mass graphs.

R_v	R_p	A_p	N_p	$U_{\min}$	U_{ht}	$F_{\max}$	k
0.6	0.25	0.1	146	0.1529	0.0016	0.2	0.26
0.6	0.25	1.0	146	−0.213	0.004	0.3	0.46
0.6	0.25	0.1	73	0.164	0.001	0.015	0.13
0.6	0.25	0.7	73	0.0388	0.0012	0.018	0.17
0.6	0.25	1.0	73	−0.0294	0.0014	0.016	0.3
0.75	0.25	0.1	73	0.4916	0.0002	0.005	0.09
0.75	0.25	1.0	73	0.2577	0.0004	0.009	0.18
0.75	0.25	0.5	146	0.3221	0.0006	0.015	0.28
0.75	0.25	1.0	146	0.1152	0.0005	0.015	0.4
0.6	0.5	1.0	73	−0.1244	0.0012	0.025	0.35
0.75	0.25	0.1	146	0.1529	0.0016	0.02	0.26

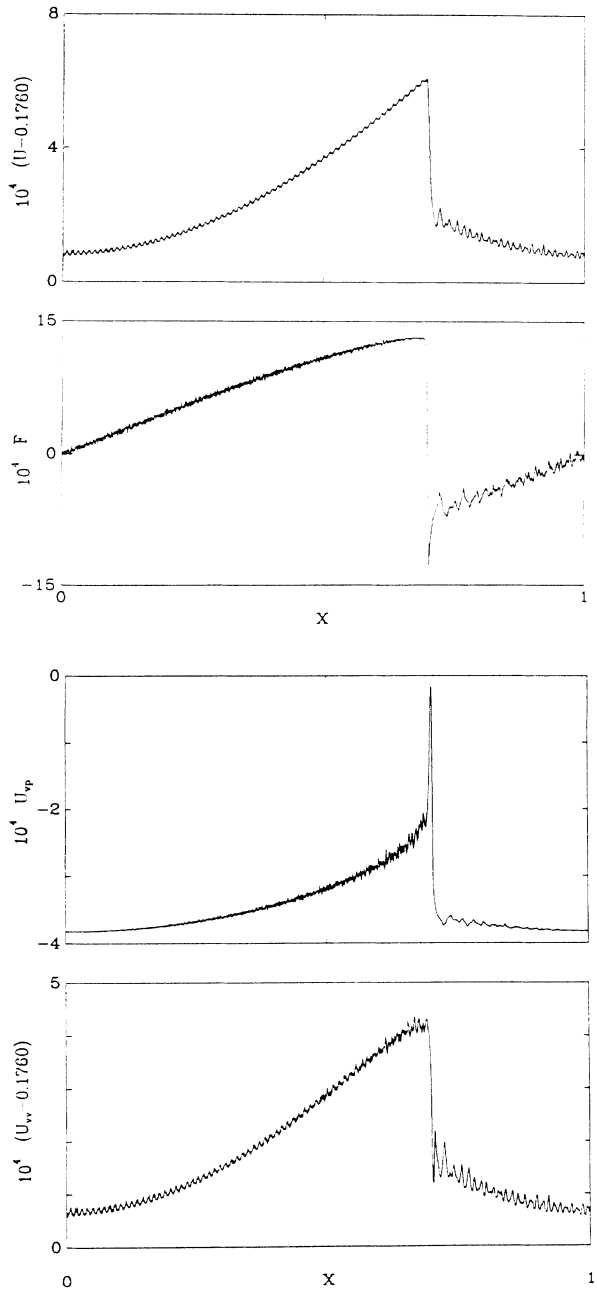

FIG. 10. The potentials and forces as a function of X for the run described in Fig. 8.

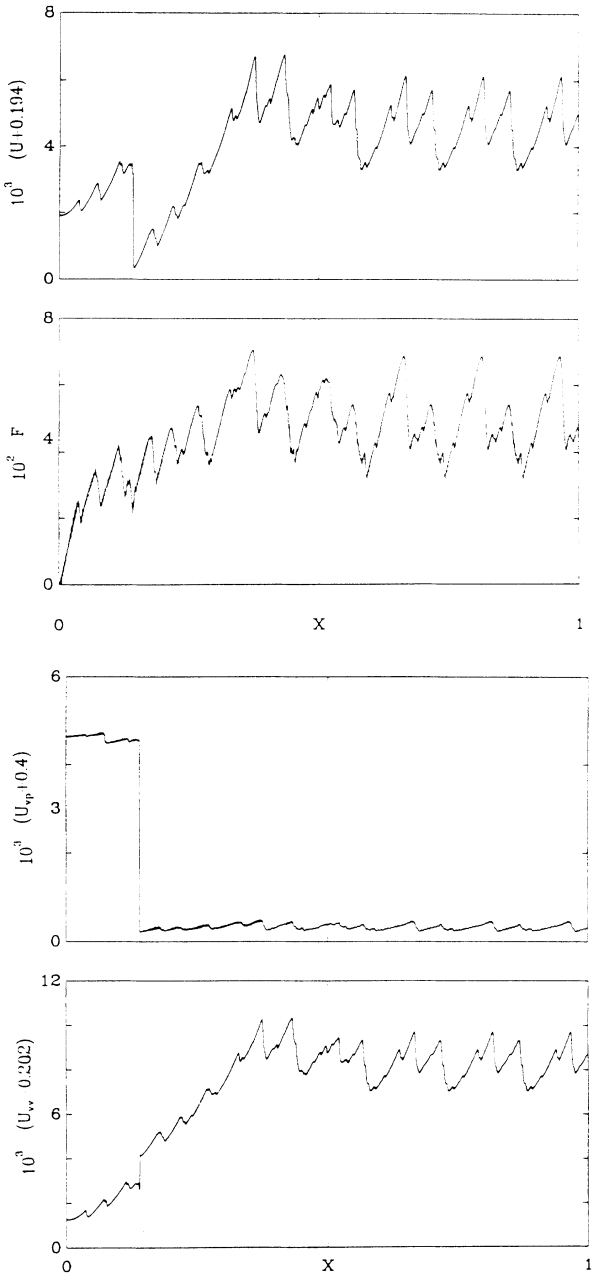

FIG. 11. The potential energy and force functions for a lattice in the plastic flow regime. $N_v = 340$, $R_v = 0.6$, $N_p = 146$, $A_p = 1.0$, and $R_p = 0.25$.

continuous. These results suggest that it is very important that further simulations be carried out on larger systems in order to test the validity of the LO theory.

IV. FINITE-SIZE EFFECTS

Figure 18 shows the variation of $A_{\text{el inst}}$ and A_{plas} as a function of system size for a given set of model parameters with a constant density of pinning centers. From Fig. 18(a) it can be seen that $A_{\text{el inst}}$ decreases with increasing system size, approximately as one over the square root of the number of vortices in the simulation. This size dependence can be understood in terms of the LO theory if $A_{\text{el inst}}$ is assumed to be equal to the pinning strength for which the size of a correlated region becomes smaller than the system size. The square-root dependence of $A_{\text{el inst}}$ implies that the crossover between the elastic and elastic instability regimes will disappear for macroscopic systems and therefore that it will not be possible to observe the elastic regime in real superconducting films. The variation of A_{plas} with system size is much weaker. Our data is consistent with a $1/\log N_v$ dependence.

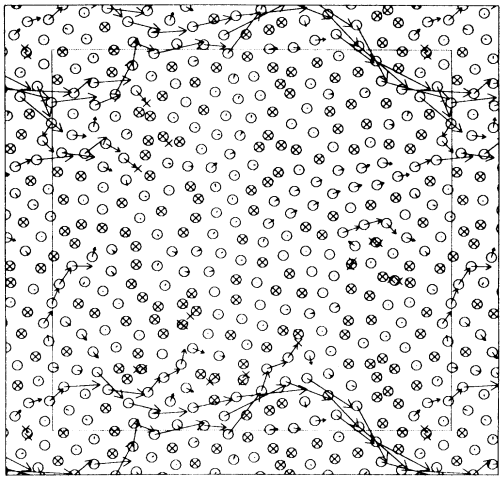

FIG. 12. Vortex motion as the lattice is shifted. Crosses mark the fixed pins and circles the vortices. The arrows show the motion of the vortices as X is increased from 0 to 0.125.

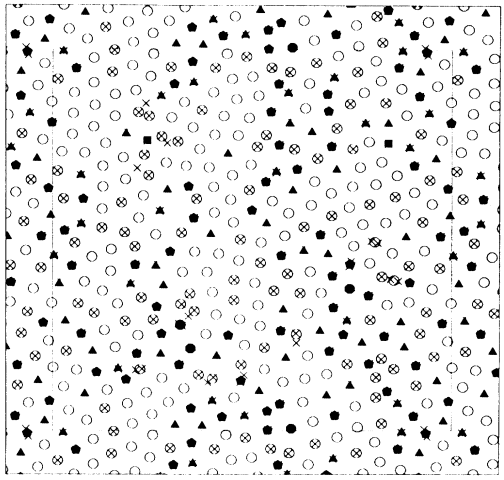

FIG. 14. The initial relaxed configuration used in the run described by Fig. 11. Crosses show the fixed pins, circles the six coordinated vortices, filled pentagons the five coordinated vortices, filled triangles the seven coordinated vortices, filled squares the four coordinated vortices, and filled octagons the eight coordinated vortices.

V. CONCLUSIONS

A. Conclusions from the simulations

In this paper we have investigated the response of the VL as it is moved over a random distribution of pinning centers in the quasistatic limit. We have been able to show that the VL exhibits three qualitatively different types of behavior as a function of the strength of the random potential. When the random potential is very weak the response of the VL is elastic and reversible. This regime is entirely due to finite size effects and should not be observable in a macroscopic sample.

As the random potential becomes stronger the pinning centers start to introduce elastic instabilities into the VL (elastic in the sense that dislocations are not created and the vortices retain the same nearest neighbors throughout the shift). Although the instabilities in this regime consist of vortex pinning-depinning events, they are the result of cooperative behavior, increasing the pinning density reduces the value of A_p at which the instabilities occur. For a macroscopic VL we would expect the elastic instabilities to be present for any arbitrarily small random potential.

As the strength of the pinning centers is increased further we begin to see topological defects introduced into the VL. Coincident with the appearance of these defects is the onset of plastic flow in the VL. The pinning centers are now strong enough to localize some of the vortices

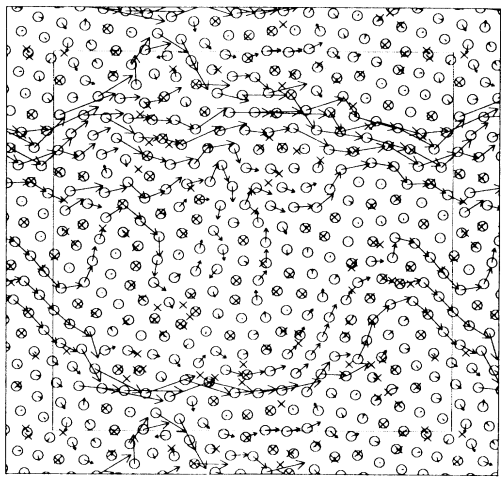

FIG. 13. The vortex flow pattern for a system with the same parameters as in Fig. 12 except that $A_p = 0.07$.

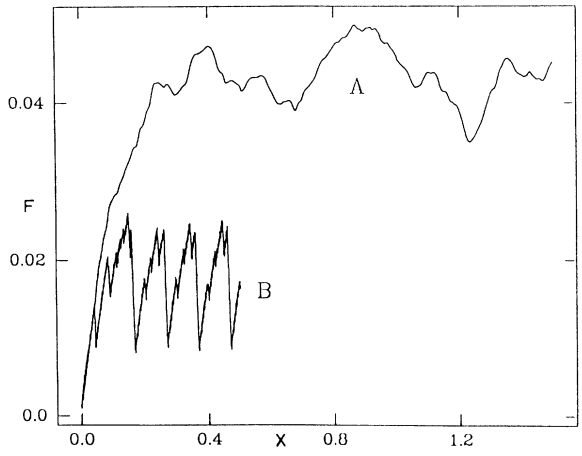

FIG. 15. The force-displacement curve $F(X)$ for two different degrees of relaxation for the same system parameters: $N_v = 340$, $R_v = 0.6$, $R_p = 0.25$, $N_p = 146$. Curve A was produced with $\delta x = 2 \times 10^{-4}$ and one relaxation per shift. Curve B was produced with $\delta x = 1 \times 10^{-4}$ and 9 relaxations per shift. Curve B does not change upon further relaxation.

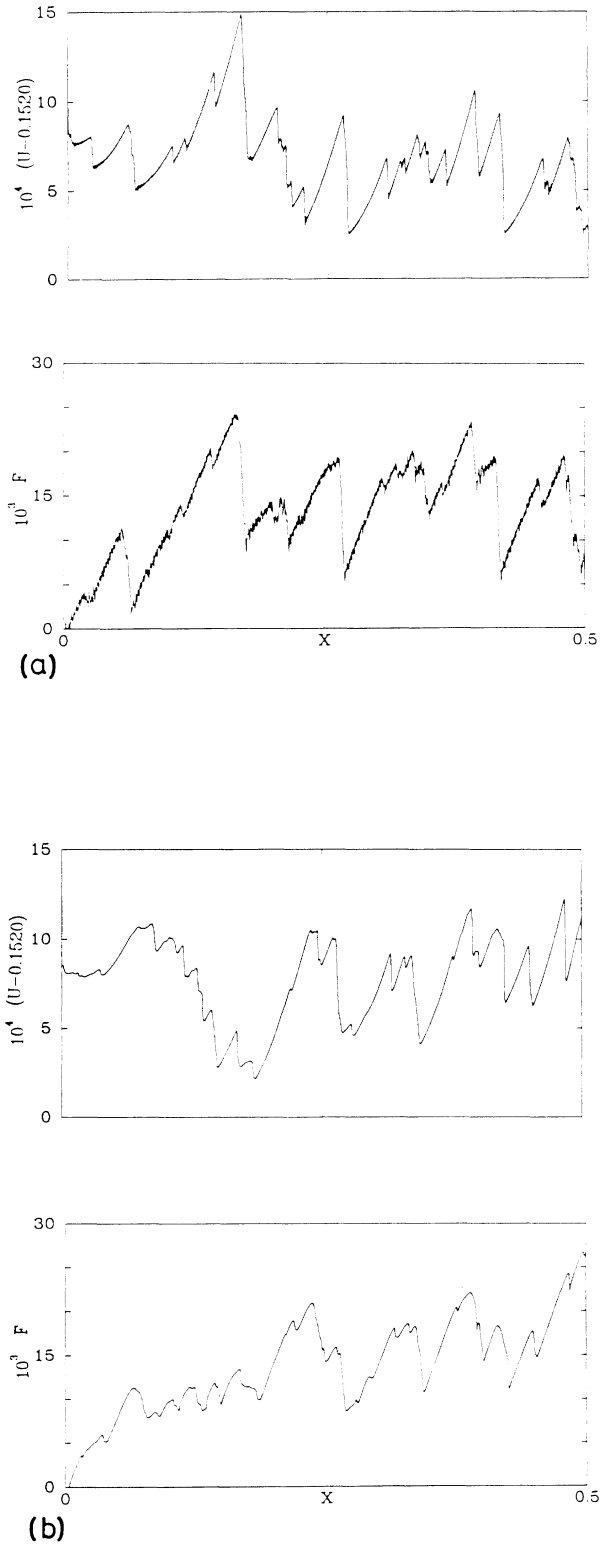

FIG. 16. A comparison between the pinning force and potential measured via (a) diffusive dynamics and (b) the successive shift and relaxation algorithm. Both runs are for a system of 340 vortices with $R_v = 0.6$, $R_p = 0.25$, $A_p = 0.1$, and $N_p = 146$.

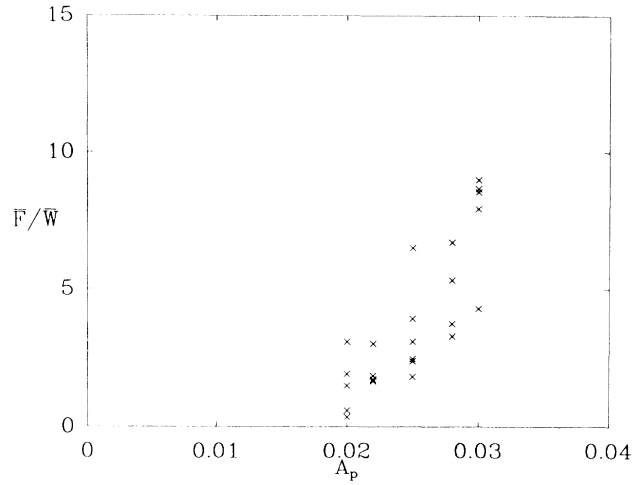

FIG. 17. $\overline{F}/\overline{W}$ plotted against A_p for a system of 340 vortices with $R_v = 0.6$, $R_p = 0.25$, and $N_p = 438$.

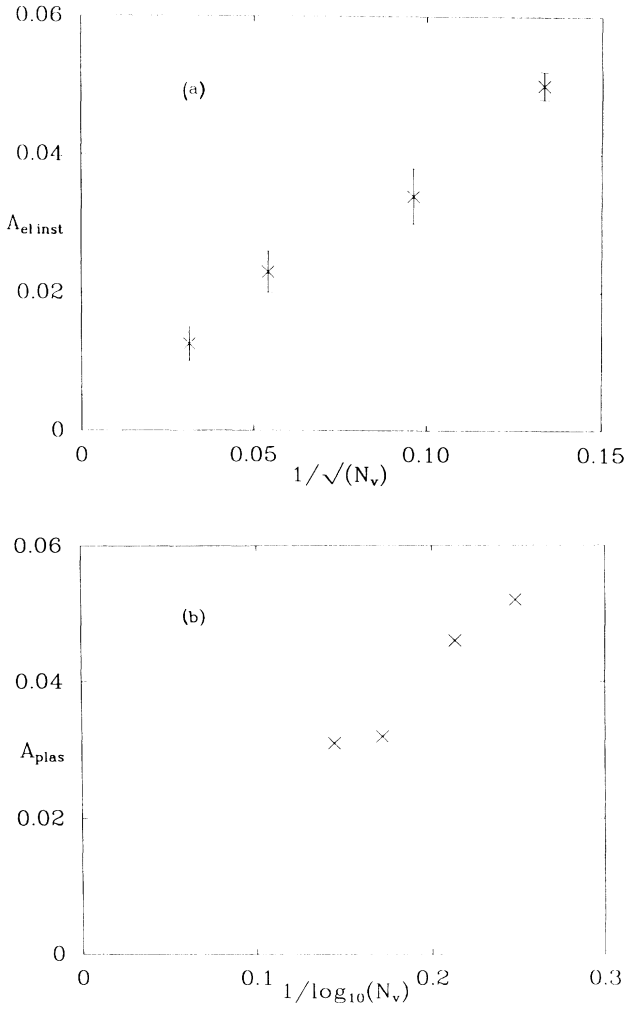

FIG. 18. (a) The variation of $A_{\text{el inst}}$ with system size, (b) the variation of A_{plas} with system size.

and the mobile vortices must flow plastically around these trapped regions. The flow is plastic as the vortices now change their neighbors as the shift proceeds. The mobile vortices flow in channels between the trapped regions. Bottlenecks in these channels result in pulsations in the vortex flow. As a result of this pulsating flow through the channels the force varies as a piecewise linear function of the center-of-mass coordinate. In this regime the random potential is strong enough to completely destroy any long-range order in the VL, the radial distributions typically decaying to unity for separations greater than four lattice spacings. As the value of A_p at which the crossover between elastic instabilities and plastic flow occurs scales only as $1/\log(N_v)$ one might expect to be able to observe both regimes in macroscopic samples.

We have also attempted to check the LO theory in our model, locating a region in parameter space where it might be expected that the LO theory should apply. However the results obtained from these simulations appear to be incompatible with those predicted by the LO theory.

The qualitative results described above were obtained for simulations of the quasistatic limit. We have also performed several simulations in which we apply a constant driving force larger than the static pinning force and in which we model the motion of the vortices using the diffusive dynamics described by Eq. (7). Although we only have preliminary results for this system, several features are already clear. First, the value of the dynamical pinning force is comparable to the static pinning force. Second, for strong pins we still the vortices flowing in channels between trapped regions (as shown in Fig. 19). Thirdly, for weak pins the distortion of the lattice is still elastic. However, in this model we seem to lose the periodic, piecewise linear form of the pinning force as a function of center-of-mass coordinate when the applied driving force is much larger than the static pinning force. These results would seem to suggest that many of the qualitative features of the VL observed in the quasistatic limit should also hold in the case where the VL motion is caused by a constant external driving force.

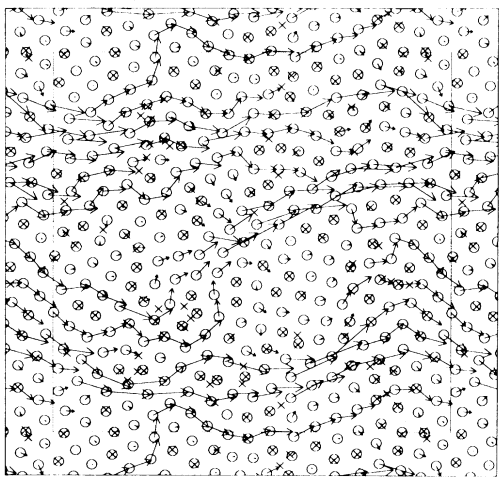

FIG. 19. Motion of the VL for a run in which a constant driving force larger than the static pinning force is applied to the VL and in which we use diffusive dynamics.

B. Connection to flux flow in type-II superconductors

The value of c_{66} for a vortex lattice in a type-II superconductor is known to vary as $b(1-b)^2$, where $b=B/B_{c_2}$ is the reduced field, B the internal field, and B_{c_2} is the upper critical field.[10] However, the strength of the pinning potential goes as $(1-b)$ (see Ref. 11). Therefore as the value of the external magnetic field is increased, the pinning potential is initially large relative to the vortex-vortex potential, then for intermediate values of b the vortex-vortex potential dominates, and finally for values of b close to 1 the pinning potential again dominates. In our simulations we can mimic the changes in the relative strengths of the pinning and vortex-vortex potentials by varying the value of A_p. If we assume that the qualitative features observed in the computer simulations will also be applicable to vortices in type-II superconductors, then we can speculate that as the external field is increased to B_{c_2}, a weakly pinned vortex lattice moves from the elastic instability regime into the plastic flow regime. This change in behavior will have several consequences. As the VL is highly defective in the plastic flow regime, we would not expect the LO theory to be valid. The crossover from elastic instabilities to plastic flow should therefore be characterized by a departure in the measured pinning force from that predicted by the LO theory. This signal has been observed experimentally.[12]

If the vortex lattice is in the plastic flow regime then, there should be some evidence that the moving vortices flow in channels between trapped regions. Several authors have suggested that the vortices do indeed flow in channels. For example analogue experiments have been performed using floating magnets in which vortex in channels was observed.[13] Flux flow in channels has also been proposed as an explanation for the noise spectrum observed in superconductors.[14] Experiments have also been performed in which weak pinning channels were specifically introduced into a strong pinning 2D superconducting sample.[15] It would be fascinating to see whether the specific structure of the mobile regions of the vortex lattice can be observed experimentally, perhaps by means of magnetic decoration techniques[16] or measurements using SQUID's (superconducting quantum interference device)[17] of various sizes.

ACKNOWLEDGMENTS

One of us (H.J.J.) would like to thank E. H. Brandt for some very illuminating and clarifying discussions, and we wish to thank Y. Brechet and C. Kallin for stimulating discussions. One of us (A.B.) is partially supported by the North Atlantic Treaty Organization (NATO) and another (H.J.J.) is partially supported by the Danish Natural Science Research Council. This work was supported by the Natural Sciences and Engineering Research Council of Canada.

[1]H. J. Jensen, A. Brass, and A. J. Berlinsky, Phys. Rev. Lett. **60**, 1676 (1988).
[2]E. H. Brandt, J. Low Temp. Phys. **53**, 41 (1983); **53**, 71 (1983); see also Phys. Rev. Lett. **50**, 1599 (1983).
[3]A. I. Larkin and Yu. N. Ovchinnikov, J. Low Temp. Phys. **34**, 409 (1979).
[4]W. F. Vinen, in *Superconducting,* edited by R. D. Parks (Marcel Dekker, New York, 1969), Vol. 2.
[5]See, for example, M. J. L. Sangster and M. Dixon, Adv. Phys. **25**, 247 (1976).
[6]R. W. Hockney and J. W. Eastwood, *Computer Simulation Using Particles* (McGraw-Hill, New York 1981).
[7]Y. B. Kim and M. J. Stephen, in *Superconductivity,* edited by R. D. Parks (Marcel Dekker, New York, 1969), Vol. 2.
[8]J. P. McTague, D. Frenkel, and M. P. Allen, in *Ordering in Two Dimensions,* edited by S. K. Sinha (North-Holland, Amsterdam, 1980).
[9]A. I. Larkin, Zh. Eksp. Teor. Fiz. **58**, 1466 (1970) [Sov. Phys.—JETP **31**, 784 (1970)]; E. H. Brandt, J. Low Temp. Phys. **34**, 375 (1986).
[10]E. H. Brandt, Phys. Rev. B **34**, 6514 (1986).
[11]E. V. Thuneberg, J. Low Temp. Phys. **57**, 415 (1984).
[12]R. Wördenweber, P. H. Kes, and C. C. Tsuie, Phys. Rev. B **33**, 3172 (1986); R. Wördenweber and P. H. Kes, *ibid.* **34**, 494 (1986).
[13]P. H. Melville, and M. T. Taylor, Cryogenics **10**, 491 (1970).
[14]J. M. A. Wade, Philos. Mag. **23**, 1029 (1971); P. Jarvis and J. G. Park, J. Phys. F **5**, 1573 (1975).
[15]A. Pruyumboom, P. H. Kes, E. van der Drift, and S. Radelaar, Phys. Rev. Lett. **60**, 1430 (1988).
[16]H. Traüble and U. Essman, Phys. Status Solidi **25**, 395 (1968).
[17]W. J. Yeh and Y. H. Kao, Phys. Rev. Lett. **53**, 1590 (1984).